What are the reference strains of *Acinetobacter baumannii* referring to?

Chantal Philippe[1 *], Adam Valcek[2, 3 *], Clémence Whiteway[2, 3], Etienne Robino[2, 3], Kristina Nesporova[3], Mona Bové[4], Tom Coenye[4], Tim De Pooter[5, 6], Wouter De Coster [7, 8], Mojca Strazisar[5, 6], Johanna Kenyon[9] and Charles Van der Henst[1, 2, 3 #]

* These authors contributed equally to the study.

[#] Corresponding author: charles.vanderhenst@vub.vib.be

Affiliations

[1] Research Unit in the Biology of Microorganisms (URBM), NARILIS, University of Namur (UNamur), Belgium.

[2] Microbial Resistance and Drug Discovery, VIB-VUB Center for Structural Biology, VIB, Flanders Institute for Biotechnology, Brussels, Belgium.

[3] Structural Biology Brussels, Vrije Universiteit Brussel (VUB), Brussels, Belgium.

[4] Laboratory of Pharmaceutical Microbiology, Ghent University, Ghent, Belgium.

[5] Neuromics Support Facility, VIB Center for Molecular Neurology, VIB, Antwerp, Belgium.

[6] Department of Biomedical Sciences, University of Antwerp, Antwerp, Belgium.

[7] Applied and Translational Neurogenomics Group, VIB Center for Molecular Neurology, VIB, Antwerp, Belgium

[8] Applied and Translational Neurogenomics Group, Department of Biomedical Sciences, University of Antwerp, Antwerp, Belgium

[9] School of Biomedical Sciences, and Infection and Immunity Program, Institute of Health and Biomedical Innovation (IHBI), Faculty of Health, Queensland University of Technology, Brisbane, Australia.

Abstract

We assembled the whole genome sequence (WGS) of a collection of 43 non-redundant modern clinical isolates and four broadly used reference strains of *Acinetobacter baumannii*. Comparison of these isolates and their WGS confirmed the high heterogeneity in capsule loci, sequence types, the presence of virulence and antibiotic resistance genes. However, a significant portion of clinical isolates strongly differ when compared to several reference strains in the light of colony morphology, cellular density, capsule production, natural transformability and *in vivo* virulence. These genetic and phenotypic differences between current circulating strains of *A. baumannii* and established reference strains could hamper the study of *A. baumannii* as an entity. The broadly used reference strains led to the current state of the art of the *A. baumannii* field, however, we propose that established reference strains in the *A. baumannii* field should be carefully used, because of the high genetic and phenotypic heterogeneities. In this study, we generated a collection of high-quality nucleotide sequences of 43 modern clinical isolates with the corresponding multi-level phenotypic characterizations. Beside the contribution of novel fundamental observations generated in this study, the phenotypic and genetic data, along with the bacterial strains themselves, will be further accessible using the first open access online platform called “Acinetobase”. Therefore, a

rational choice of modern strains will be possible to select the ones that suit the needs of specific biological questions.

Introduction

Antibiotics overuse, along with fewer new therapeutics, represents a major challenge for human health (Hernando-Amado et al., 2019; Poirel and Nordmann, 2006). Multidrug-resistant (MDR) bacteria are increasingly isolated around the world, leaving physicians increasingly facing no therapeutic option (Murray et al., 2022). As a direct consequence, patients are currently dying from previously treatable diseases. In this context, WHO and CDC prioritize problematic bacterial pathogens for which antibiotic resistance significantly impacts human health (Centers for Disease Control, 2019; Tacconelli et al., 2018). *Acinetobacter baumannii* (Whiteway et al., 2022), a member of the ESKAPE multidrug-resistant and most problematic nosocomial pathogens (de Oliveira et al., 2020), was designated as a top-priority and critical agent for which therapeutic alternatives are urgently required (Tacconelli et al., 2018).

A. baumannii is a Gram-negative opportunistic bacterial pathogen that thrives in hospital settings, especially in intensive care units where weakened patients are treated (Whiteway et al., 2022). Beside their intrinsic and acquired antibiotic resistance, *A. baumannii* resistance to desiccation and disinfectants render any decontamination strategy a real challenge (Chiang et al., 2018). One key aspect sustaining the rapid spread of antibiotic resistance amongst *A. baumannii* isolates is their natural competence (Vesel and Blokesch, 2021). *A. baumannii* bacteria undergo horizontal gene transfer during which exogenous DNA is taken up and integrated within the bacterial genome (da Silva and Domingues, 2016). As a direct consequence, rapidly evolving *A. baumannii* bacteria show a dynamic genome, with an estimated core (conserved) genome of only 16.5%, while 25% of the genome is unique to each

strain, having no counterpart in any other *A. baumannii* genome (Imperi et al., 2011). However, despite their clinical relevance, *A. baumannii* bacteria remain poorly understood. Especially, their virulence and non-antibiotic associated resistance still needs to be better characterized (Harding et al., 2017).

One possible explanation for this gap of knowledge is the heterogeneity amongst *A. baumannii* isolates, rendering the multiple approaches of typing of this bacterial species difficult, with as a proof-of-concept the huge diversity of the polysaccharide capsules and the outer core of the lipooligosaccharide (LOS) in *A. baumannii*, in addition to the two multilocus sequence typing (MLST) schemes (Gaiarsa et al., 2019). The LOS is present in *A. baumannii* instead of the common lipopolysaccharide (LPS). Unlike LPS, the LOS is lacking the O-antigen and is composed of lipid A with variable amounts of inner and outer core sugars (Kenyon et al., 2014). The outer sugars of LOS show diversity across strains, dependent on glycosyltransferases and nucleotide-sugar biosynthesis enzymes encoded in a highly variable outer core locus (OCL) (Geisinger et al., 2019). The LOS, a major virulence component in Gram-negative bacteria is encoded chromosomally and to date 14 variants (differing in the presence or absence of genes encoding multiple glycosyltransferases and other enzymes) were described. OCL types can be divided in two groups (A or B) based on the presence of *pda1* and *pda2* genes (Kenyon et al., 2014). The OCL consists of genes involved in the synthesis, assembly and export of complex oligosaccharides that are then linked to lipid A to form the LOS (Kenyon and Hall, 2013). Bacterial capsule consists of a polysaccharide layer deposited as the outermost surface exposed leaflet on prokaryotic cells, impacting the virulence and antibiotics, as well as non-antibiotics-based resistances (Dong et al., 2006; Niu et al., 2019). The locus encoding the genes involved in the production and the assembly of the polysaccharide capsule (KL) is chromosomally encoded and typically ranges from 20 to 35 kb in size. Its genetic organization comprises three modules (Kenyon and Hall, 2013) encoding (i) the export machinery consisting of three

proteins; Wza, Wzb, and Wzc, (ii) glycosyltransferases and the capsule processing genes (and optionally genes for the synthesis and modification of complex sugars) and (iii), genes involved in the synthesis of simple sugar substrates.

Witnessing the high diversity amongst *A. baumannii* isolates, our approach aims at investigating to which extend the use of reference strains actually reflects the dynamic nature and intrinsic heterogeneity of these bacteria in general, at the phenotypic and genotypic level. In this study, we assessed the phenotypic and genetic diversity levels of 43 *A. baumannii* modern clinical isolates, and we compared them to established type strains of *A. baumannii* in the field: AB5075, ATCC17978, ATCC19606 and DSM30011, which are widely used in various studies (Bravo et al., 2016; de Silva et al., 2017; Jacobs et al., 2014; Roussin et al., 2019).

Materials and Methods

Modern clinical isolates, reference strains and phylogeny inference

A non-redundant collection of 43 modern (not older than 8 years) clinical isolates from the National Reference Center for Antibiotic-Resistant Gram-Negative Bacilli (CHU UCL-Namur) and four established reference strains: ATCC17978-VUB, ATCC19606-VUB, DSM30011-VUB and AB5075-VUB were studied. The reference strains AB5075, ATCC17978 and ATCC19606 are non-MDR (except AB5075) strains of clinical (osteomyelitis, meningitis and urine, respectively) origin (Gallagher et al., 2015; Harding et al., 2017) while DSM30011 is a non-MDR environmental strain obtained from plant microbiota (Repizo et al., 2017). The reference strains were designated with the extension "-VUB" in order to distinguish the strains and their sequences examined within our study. The selected isolates were described in our previous study (Valcek et al., 2021). In order to increase the heterogeneity of the collection, three carbapenem-susceptible isolates (AB21-VUB, AB169-VUB and AB179-VUB) were

119 added and analyzed as well. We sequenced the whole genome of these isolates using shorts
120 reads (Illumina) combined with long reads [Oxford Nanopore Technologies (ONT)] sequencing
121 techniques to generate *de novo* assembled genomes for each of them.
122
123 **Short- and long-read sequencing**
124 Genomic DNA extraction and the sequencing library preparation for short-read 2x250 bp
125 paired-end MiSeq (Illumina) sequencing was performed as described before (Valcek et al.,
126 2021). The DNA for long-read MinION (ONT) sequencing was extracted using Genomic-tip
127 100/G (Qiagen, Hilden, Germany). The long-read sequencing libraries were prepared using 1D
128 Ligation Barcoding Kit (SQK-LSK109 and EXP-NBD104 ONT, Oxford, UK). Samples were
129 QCed using Qubit (dsDNA BR chemistry, Thermo Fisher Scientific), and Fragment Analyzer,
130 Agilent Technologies (using DNF-464 kit). Average size of the fragments was 45-70 kb.
131 Samples were equimolarly pooled and run per 12 in one run which was always 2x reloaded.
132 MinION flowcells had min. 1200 sequencable pores at the start and initial loading was
133 approximately 35 fmol followed by 2 reloads each after 24h into sequencing. The sequencing
134 was performed on MinION Mk1b (ONT) using R9.4.1 (FLO-MIN106) flowcells.
135
136 **Sequence data analysis**
137 The long-reads sequences were demultiplexed and basecalled using Guppy v3.2.2 and
138 subsequently were adaptor, quality (Q≤13) and length (5000 bp) trimmed using Porechop
139 v0.2.2 (https://github.com/rrwick/Porechop) and NanoFilt v2.8.0 (de Coster et al., 2018.),
140 respectively. The short reads (BioProject PRJNA734485) were used to polish the long reads
141 employing Ratatosk v0.7.0 (Holley et al., 2021). The corrected reads were then assembled using
142 Flye v2.9 (Kolmogorov et al., 2019) resulting in circular chromosomal contigs of all isolates.
143 The circularity was verified by mapping short reads to corresponding assemblies in order to

observer overlapping sequences. The circular chromosomal contigs were polished using long reads via racon v1.4.20 (https://github.com/isovic/racon) and Medaka v1.2.2 (https://github.com/nanoporetech/medaka) and subsequently by quality (Q≤20) and adaptor trimmed (using Trimmomatic (Bolger et al., 2014)) short reads in three rounds of Pilon (Walker et al., 2014) polishing.

Antimicrobial resistance genotype and phenotype

The antimicrobial susceptibility testing and characterization of its genetic background was performed and described in our previous study (Valcek et al., 2021).

Natural competence of the isolates

The natural competence of the clinical isolates and reference strains of *A. baumannii* was assessed by starting an overnight bacterial culture from -80°C stock in 5mL of LB (37°C at 160 rpm). The culture was diluted 1:100 in 2mL microtube (10µL of the bacterial culture + 990µL tryptone solution of 5g/L). Then 3µL of the diluted culture was mixed with 3µL of plasmid DNA (100ng/µL) in 1mL microtube. Subsequently, 3µL of the mix of culture and plasmid DNA was transferred to a 2mL microtube containing 1mL tryptone 5g/L agar 2%. A 3µL of diluted bacterial culture without plasmid DNA was used as a negative control.

After 6h incubation at 37°C, 100µL of tryptone solution at 5g/L was added to the microtube with the culture and plasmid DNA and vortexed gently. A 50µL of the suspension was plated on LB agar plates containing apramycin (50µg/mL) to select transformants. The negative control was plated apramycin LB agar plates too. Colonies were counted after overnight incubation at 37°C.

Hemolytic and protease activities

To assess the potential hemolytic activities of the different *A. baumannii* isolates, we spotted 5 µl of an O/N (overnight) culture of bacteria previously grown in LB medium for 16 hours at 37°C under constant agitation (175 rpm) on 4 different Blood Agar Plates: (i) Columbia Agar with 5% Horse Blood, (ii) Columbia Agar with 5% Sheep Blood, (iii) Trypticase™ Soy Agar II with 5% Horse Blood and (iv) Trypticase™ Soy Agar II with 5% Sheep blood, all purchased from BD (Becton, Dickinson and Company, Franklin Lakes, NJ). To test for secreted protease activity, we used the same approaches as described above and spotted the 5 µl of bacteria on LB agar plates containing 2% of Skim Milk Powder for microbiology (Sigma-Aldrich/Merck KGaA, Darmstadt, Germany). Plates were incubated at 25°C and monitored for hemolytic and protease activities after 1, 2 and 6 days of incubation.

Phylogenetic analysis

The maximum-likelihood tree depicting the relatedness of the isolates was constructed from assembled complete genomes using precited open reading frames obtained by Prokka (Seemann, 2014) as an input for the core-genome alignment created using Roary (Page et al., 2015). RAxML (Stamatakis, 2006) was used for calculation of the phylogenetic tree using general time reversible with optimization of substitution rates under GAMMA model of rate heterogeneity method supported by 500 bootstraps. The phylogenetic tree was visualized in iTOL (Letunic and Bork, 2019).

Genotypic characterization

The resistance and virulence genes were detected using ABRicate (https://github.com/tseemann/abricate) employing ResFinder 4.1 (Bortolaia et al., 2020), VFDB 2022 (Liu et al., 2022) and MEGARes 2.0 (Doster et al., 2020) databases, respectively with 90% threshold for both gene identity and coverage. The typing of capsule-encoding loci

(KL) and lipooligosaccharide outer core (OCL) were determined using Kaptive (Wick et al., 2018; Wyres et al., 2020) after manual curation of the corresponding loci by mapping the short reads on anticipated reference sequence of the KL using Geneious R9 (Biomatters, NZ).

Macrocolony morphology

5 µl of overnight bacterial suspension (~ $1x10^8$ cells) was plated on Columbia Agar with 5% Sheep Blood purchased from BD (Becton, Dickinson and Company, Franklin Lakes, NJ). The plates were incubated non-inverted for 24h at 25°C and subsequently photographed by a Canon® camera.

Capsule production

1 ml of overnight culture in a 1.5 ml microtube was centrifuged for 2 min at 7000 rcf. The supernatant was removed, and the pellet was resuspended in 1 ml of PBS. Subsequently, 875 µl of PBS resuspended bacteria were mixed with 125 µl of LUDOX® LS colloidal silica (30 wt. % suspension in H_2O, Merk) (Ardissone et al., 2014; Kon et al., 2020). This mix was then centrifuged for 30 min at 12.000 rcf and immediately photographically recorded.

Transmission electron microscopy (TEM)

Transmission electron microscopy (TEM) was used for direct capsule visualization by labeling the capsule of 11 *A. baumannii* isolates, 9 modern clinical isolates and 3 reference strains, which ranges from high to low densities. The fixation and staining of the bacteria were performed as described before (Chin et al., 2018). The cupule with the fixed pellet of bacteria (polymerized for 5 hours) was embedded in resin and polymerized (12h at 37°C, 48h at 45°C and 3 days at 60°C). The ~60 nm slides of the resin were marked with acetate uranyl and placed on the electron microscopy grid.

Virulence in *Galleria mellonella* model of infection

TruLarv research grade larvae of *G. mellonella* (BioSystems Technology) were stored at 15°C no longer than 5 days after arrival and were incubated for 30 min at 4°C prior to injection. Bacteria from an overnight culture were washed with physiological saline (PS) (0.9% NaCl) and diluted to approx. $1x10^7$ CFU/ml. The larvae were injected with 10 µl of PS containing $1x10^5$ CFU/ml of *A. baumannii* in the last left proleg using a 0.3 ml insulin syringe (BD MicroFine). Each of the nine selected strains of *A. baumannii* were injected into 10 larvae and 10 larvae were injected with PS as a negative control. The experiments were carried in duplicates and the survival (assessed by keratinization and mobility) rate was evaluated each day in a period of 5 days.

Results

Genotypical characterization of the isolates

We have previously described the sequence types (ST) and the antibiotic resistance profiles of 40 modern carbapenem-resistant clinical isolates of *A. baumannii* bacteria (Valcek et al., 2021). We completed our strain collection by generating the whole genome sequence (WGS) of three carbapenem-sensitive modern isolates (AB21-VUB, AB169-VUB and AB179-VUB) and four broadly used reference strains in the *A. baumannii* field (AB5075-VUB, ATCC19606-VUB, ATCC17978-VUB and DSM30011-VUB), their phylogenetic tree and antimicrobial resistance genes (Supplementary Figure 1).

We further investigate the genetic background of our extended strain collection and generate polished *de novo* assembled genomes by combining Illumina and Oxford Nanopore Technologies sequencing data. Comparison of the whole genome sequences (WGS) of the 43 modern clinical isolates and four reference strains of *A. baumannii*, identified a core genome

containing 2009 genes (Figure 1), representing 14.76% of coding sequences (CDS) from the pan-genome of 13611 CDS. The more *A. baumannii* genomes are analyzed, the more unique genes are identified (Figure 2B) while the number of conserved genes decreased. These findings confirm the great variability of *A. baumannii* bacteria, pointing towards a still open pan-genome of *A. baumannii* bacteria that are often changing. Therefore, we still make the current prediction that, every time a new isolate of *A. baumannii* is sequenced, most likely (a) novel gene(s) would be identified.

We further analyzed the 47 genomes of our strain collection in regard to their respective sequence type (ST), capsule locus type (KL) and lipooligosaccharide locus (OCL) types. Twelve ST groups were identified, with ST2 as the most prevalent (25/43) followed by ST636 (6/43), ST1 (4/43), ST85 (2/43), ST78 (2/43) and ST604, ST215, ST158 and ST10 (one isolate each) (Figure 2). The four reference strains belong to ST1 (AB5075-VUB), ST52 (ATCC19606-VUB), ST437 (ATCC17978-VUB) and ST738 (DSM30011-VUB). We found that the most frequent capsule type was KL40 (10/43) followed by KL9 (6/43), KL3 (5/43), KL2 (4/43), KL13 and KL4 (3/43), KL22 and KL6 (2/42) and KL125, KL124, KL81 KL58, KL18, KL12, KL10 and KL7 (one isolate each) (Figure 2). We confirmed that the reference strains ATCC19606-VUB and ATCC17978-VUB, both belonged to KL3, while DSM30011-VUB to KL47 and AB5075-VUB to KL25 (Arbatsky et al., 2015; Senchenkova et al., 2015; Wang-Lin et al., 2017). In this regard, the reference strains ATCC19606-VUB and ATCC17978-VUB, both KL3, were more representative than DSM30011-VUB (KL47) and AB5075-VUB (KL25) which were sole to be of said KL. The typing of the locus encoding the OCL of the LOS revealed high occurrence of OCL1 (31/43) followed by OCL2 (7/43), OCL6 and OCL3 (2/43) and OCL5 (1/43). We confirmed that the reference strains belonged to OCL2 (AB5075-VUB and ATCC17978-VUB), OCL3 (ATCC19606-VUB) and OCL6 (DSM30011-VUB).

The phylogenetic along with the genetic analyses of KL and OCL showed that, except for AB5075-VUB, the reference strains ATCC17978-VUB, ATCC19606-VUB and DSM30011-VUB only clustered with the clinical isolates of rare ST and KL. Despite AB5075-VUB was sole of the KL25 it clustered closer to the modern clinical isolates of *A. baumannii*. In addition, a variety of genes from operons encoding RND efflux pumps involved in virulence were not present in said three oldest reference strains (ATCC19606-VUB, ATCC17978-VUB and DSM30011-VUB), and a key gene involved in biofilm formation (*bap*) was undetected in all reference strains (Figure 2). Employing MEGARes 2.0 database, only reference strain AB5075-VUB encoded all three RND efflux pumps *adeIJK, adeABC,* and *adeFGH*, while DSM30011-VUB, ATCC17978 and ATCC19606-VUB had an incomplete *adeABC* (lacking *adeC*, all three strains) and/or *adeFGH* (lacking *adeF*, DSM30011-VUB, ATCC19606-VUB) operon. Besides these three reference strains, only six modern clinical MDR strains of *A. baumannii* contained one or more incomplete operons encoding RND efflux pumps.

Figure 1 and 2. Bottom of the file (horizontally oriented)

Natural competence of *A. baumannii* clinical isolates and strains

We next assessed the natural competence ability of all the *A. baumannii* strains. The reference strain AB5075-VUB was used as a positive control due to its high competence in the tested conditions (Le et al., 2021). We have categorized the strains in regard to its level of competence (Table 1). These results are showing not only variability in the natural competence of the clinical isolates and reference strains of *A. baumannii*, but also a different level of the natural competence.

Table 1: A table summarizing number of colonies of *A. baumannii* clinical isolates and reference strains detected after the transformation with plasmid containing apramycin cassette. High: >50 colonies; Medium: 30 – 50 colonies; Low: <5 colonies; Not detected – 0 colonies; in the tested conditions. ND – Not Detected.

Strain	Level of competence	Strain	Level of competence
DSM30011-VUB	Medium	AB181-VUB	ND
ATCC17978-VUB	ND	AB183-VUB	ND
ATCC19606-VUB	ND	AB186-VUB	High
AB3-VUB	ND	AB187-VUB	ND
AB9-VUB	ND	AB188-VUB	Low
AB14-VUB	ND	AB189-VUB	High
AB16-VUB	ND	AB193-VUB	ND
AB20-VUB	High	AB194-VUB	ND
AB21-VUB	ND	AB212-VUB	ND
AB32-VUB	Low	AB213-VUB	ND
AB36-VUB	ND	AB214-VUB	ND
AB39-VUB	ND	AB216-VUB	ND
AB40-VUB	ND	AB217-VUB	ND
AB167-VUB	ND	AB219-VUB	ND
AB169-VUB	High	AB220-VUB	ND
AB171-VUB	ND	AB222-VUB	High
AB172-VUB	ND	AB224-VUB	ND
AB173-VUB	ND	AB226-VUB	ND
AB175-VUB	ND	AB227-VUB	High
AB176-VUB	High	AB229-VUB	High
AB177-VUB	ND	AB231-VUB	ND
AB179-VUB	ND	AB232-VUB	High
AB180-VUB	ND	AB233-VUB	ND

Colony morphology of *A. baumannii* and the need for classification to define new phenotypic categories

We have now confirmed the high heterogeneity at the genetic level amongst our strain collection of MDR modern clinical isolates (Figure 1). To test whether this observation correlates with different levels of phenotypic heterogeneity, we spotted each strain on different

304 blood and milk derived media and observed the potential hemolytic or secreted protease
305 activities (Van der Henst et al., 2018) as well as the ultrastructure of macrocolonies (Figure 3).
306 The clinical isolates and the reference strains did not show detectable hemolytic or protease
307 activities in the tested conditions, which is a common trait amongst *A. baumannii* bacteria
308 (Bouvet and Grimont, 1986) (Figure 1). The reference strains AB5075-VUB, DSM30011-
309 VUB, ATCC17978-VUB and ATCC19606-VUB do represent this common phenotypic trait,
310 despite the high genetic diversity observed, confirming that the tested modern clinical isolates
311 did not acquire increased hemolytic nor secreted protease activities. However, the analysis of
312 the macrocolonies morphology highlights an important diversity level of the modern clinical
313 isolates compared to the reference strains. As shown in Figure 3 and Table 2, we observed at
314 least five different categories of ultrastructure of macrocolony for the modern clinical isolates
315 and only two categories for the tested reference strains, with the more modern isolate AB5075-
316 VUB being different compared to the three other reference strains DSM30011-VUB,
317 ATCC17978-VUB and ATCC19606-VUB. We could identify six constitutive mucoid strains
318 in the macrocolony type (MT) "A" group of *A. baumannii* isolates (Figure 3B). The colonies
319 of the isolates with constitutive mucoid phenotype had circular shape and smooth margin. The
320 least frequent morphology of a colony and second most mucoid was circular with raised top of
321 darker white color with only three isolates, representing the MTB group (Figure 3B). The most
322 abundant (n=17) type of colony (MTC) was irregular with translucent bottom and opaque top
323 with irregular margin. This group also includes the most modern reference strain AB5075-VUB
324 (Figure 3A). The isolates of the MTD group (n=14) produced circular colonies with undulate
325 margin and volcano shaped center. Most of the reference strains belongs to the MTE group of
326 seven least mucoid isolates (Figure 3B) with circular shape, translucent center and opaque outer
327 ring. Hence, the shapes of the colonies allowed to divide the isolates into five macrocolony type
328 groups with one representative isolate depicted in Figure 3 (Table 2).

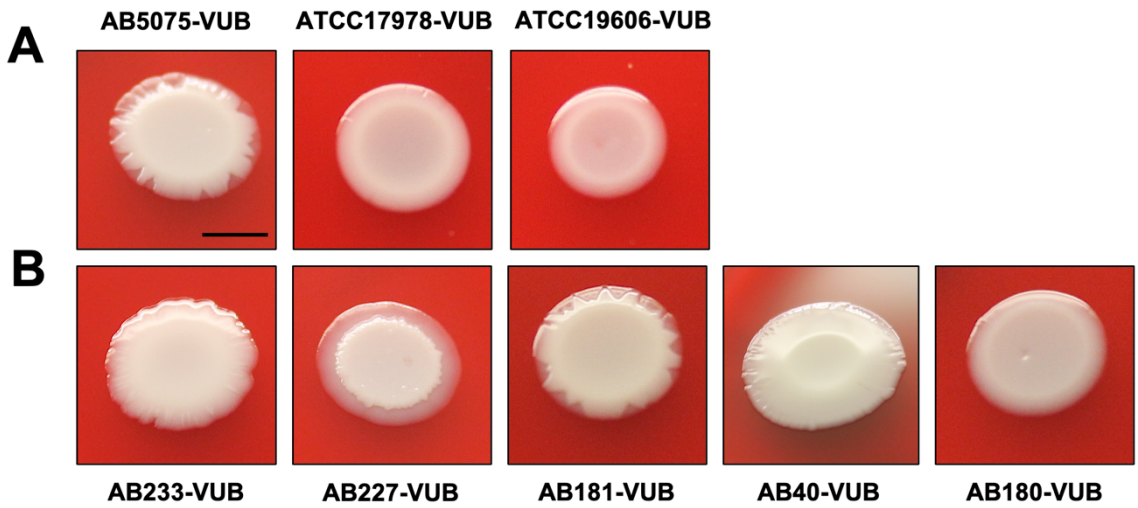

Figure 3: Diversity of the macrocolony types of the reference strains (A) compared to modern clinical isolates (B) grown on columbia agar plates with 5% sheep blood. Scale bar: 1 cm.

Table 2: A table dividing the reference strains and the clinical isolates to five categories (MTA-MTE) based on the colony morphology from the most mucoid phenotype (A) to the least mucoid phenotype (E). Each category is represented by one isolate, which is depicted in Figure 3B.

Macrocolony Type (MT)	AB233-VUB **(MTA)**	AB227-VUB **(MTB)**	AB181-VUB **(MTC)**	AB40-VUB **(MTD)**	AB180-VUB **(MTE)**
	AB3-VUB	AB16-VUB	AB14-VUB	AB9-VUB	AB32-VUB
	AB39-VUB	AB20-VUB	AB21-VUB	AB36-VUB	AB212-VUB
	AB173-VUB		AB169-VUB	AB167-VUB	AB213-VUB
	AB177-VUB		AB171-VUB	AB175-VUB	ATCC17978-VUB
			AB172-VUB	AB176-VUB	ATCC19606-VUB
			AB186-VUB	AB179-VUB	DMS30011-VUB
			AB188-VUB	AB183-VUB	
			AB193-VUB	AB187-VUB	
			AB194-VUB	AB189-VUB	
			AB217-VUB	AB214-VUB	
			AB219-VUB	AB216-VUB	
			AB220-VUB	AB222-VUB	
			AB224-VUB	AB226-VUB	
			AB229-VUB		
			AB231-VUB		
			AB232-VUB		
			AB5075-VUB		

Capsule production of *A. baumannii*

As the mucoid phenotype can reflect the presence of an abundant polysaccharide capsule surrounding bacteria, we established a density gradient assay to assess encapsulation level of all *A. baumannii* isolates in a medium to high throughput level (Figure 4) (Whiteway et al., 2021). In this phenotypic assay, low density bacteria have a high capsulation level, while denser bacteria have lower capsulation levels (Figure 4A). A high heterogeneity degree concerning the density of *A. baumannii* bacteria, crossing the full range from low to high density levels is observed (Figure 4D). Interestingly, four clinical isolates were divided into two fractions, suggesting diversity in production of CPS even within the same isolate, possibly pointing towards a high frequency of phase variation leading to phenotypic heterogeneity previously described (Tipton et al., 2015). In majority, the reference strains show high densities except for AB5075-VUB characterized by a medium density level. Despite having low capsulation levels, the ATCC19606-VUB isolate constantly shows a lower density compared to the strain ATCC17978-VUB. On the other hand, none of the high-density isolates belonged to KL40, unlike majority of low-density producers, pointing towards causality. While in high density isolates no other pattern than frequent occurrence of ST2 (10/15) was observed, the isolates of low density were often of KL40 (7/9) of ST2 (5/9) or ST636 (4/9). In conclusion, we could not attribute a specific cell density with the capsule type. The colony morphology (MTE) and the density gradient of four modern clinical isolates of our collection (AB32-VUB, AB180-VUB, AB212-VUB and AB213-VUB) resembles those of the low capsulated reference strains ATCC17978-VUB, ATCC19606-VUB and DSM30011-VUB, hence was to a certain extent represented by two reference strains. In this regard, the reference strain AB5075-VUB represented 17 clinical isolates of MTC, yet the density gradients of this group were too heterogenous to be represented by a sole reference strain AB5075-VUB. However, the majority (n=22/43) of the modern clinical isolates was not represented by the reference strains of *A. baumannii* considering the capsule production (density gradient) and macrocolony types.

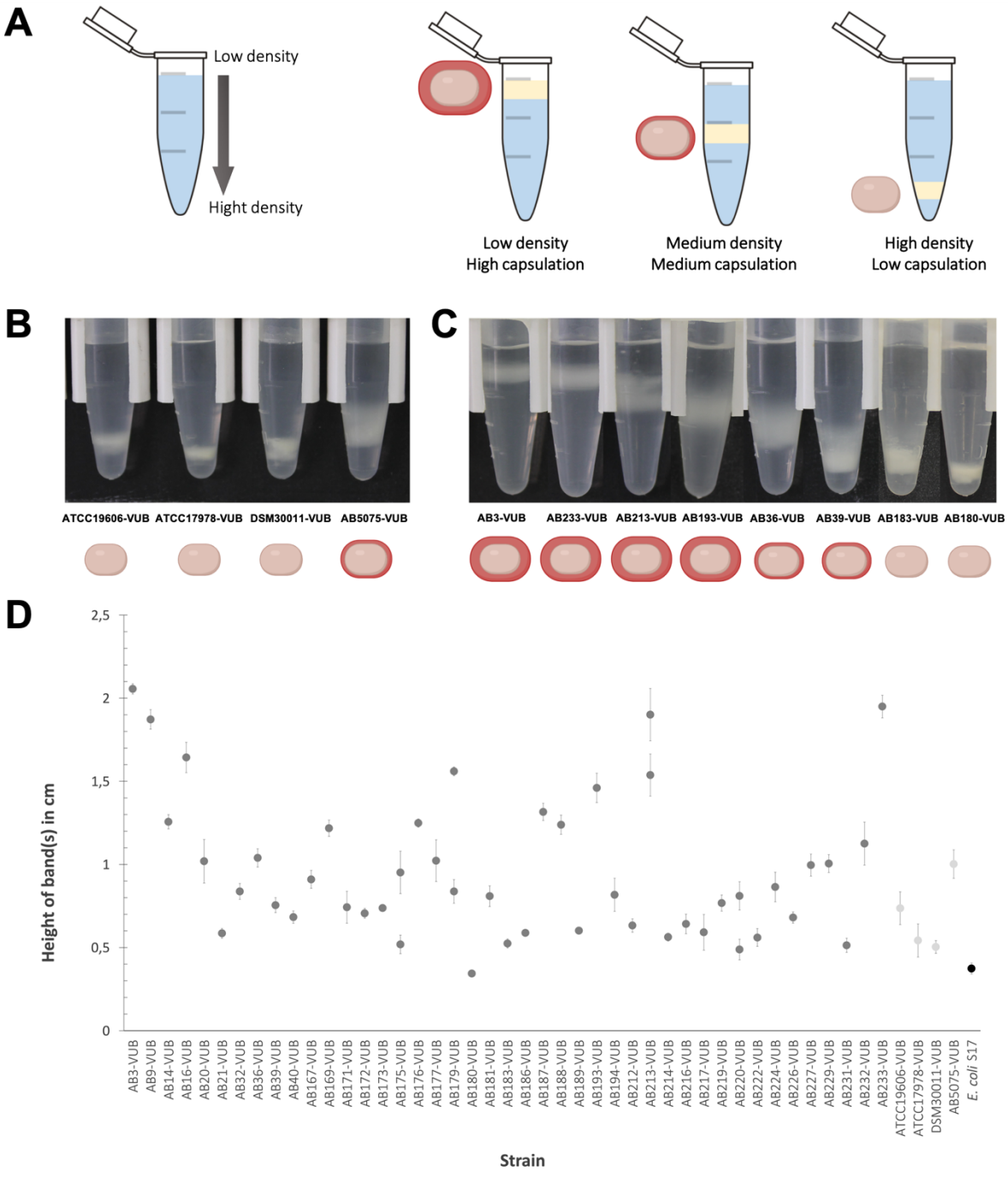

364

365 **Figure 4:** (A) Depiction of the density gradient measuring principle. (B) Capsulation level of the reference strains
366 and (C) comparison of various levels of capsulation of the modern clinical strains of *A. baumannii*. (D)
367 Quantification of the density of bacterial cells measured in a gradient colloidal silica; standard deviation was
368 calculated from biological triplicates.

369

To directly observe capsule deposition and thickness at high resolution and at the single cell level, we combined capsule labeling with transmission electron microscopy (TEM) approach (Figure 5). As expected, high density bacteria are surrounded by a denser and thicker capsule compared to low density bacteria (Figure 5B). Concerning the reference strains, we confirm AB5075-VUB to be the more capsulated reference strain tested in this study. We could not detect any capsule deposition on the ATCC17978-VUB strain and the ATCC19606-VUB shows weak and heterogeneously deposited layer in the tested conditions. This is in line with the reference strain ATCC19606-VUB being less dense compared to the reference strain ATCC17978-VUB in our density gradient assay (Figure 4D). Two less capsulated modern strains, the AB180-VUB and AB183-VUB also show high densities (in density gradient assay) with less abundant capsule deposition. The least dense isolates AB3-VUB, AB193-VUB and AB213-VUB show a high abundance of capsule formation. Accordingly, the strains AB36-VUB that shows an intermediate density level have an intermediate capsule deposition level while the AB39-VUB strain reaches a higher density with less capsule deposition. Taken together, these data show that bacterial density correlates with capsule abundance of *A. baumannii* bacteria and that the reference strains does not show all the heterogeneity observed in the modern clinical isolates tested regarding capsule production level.

388

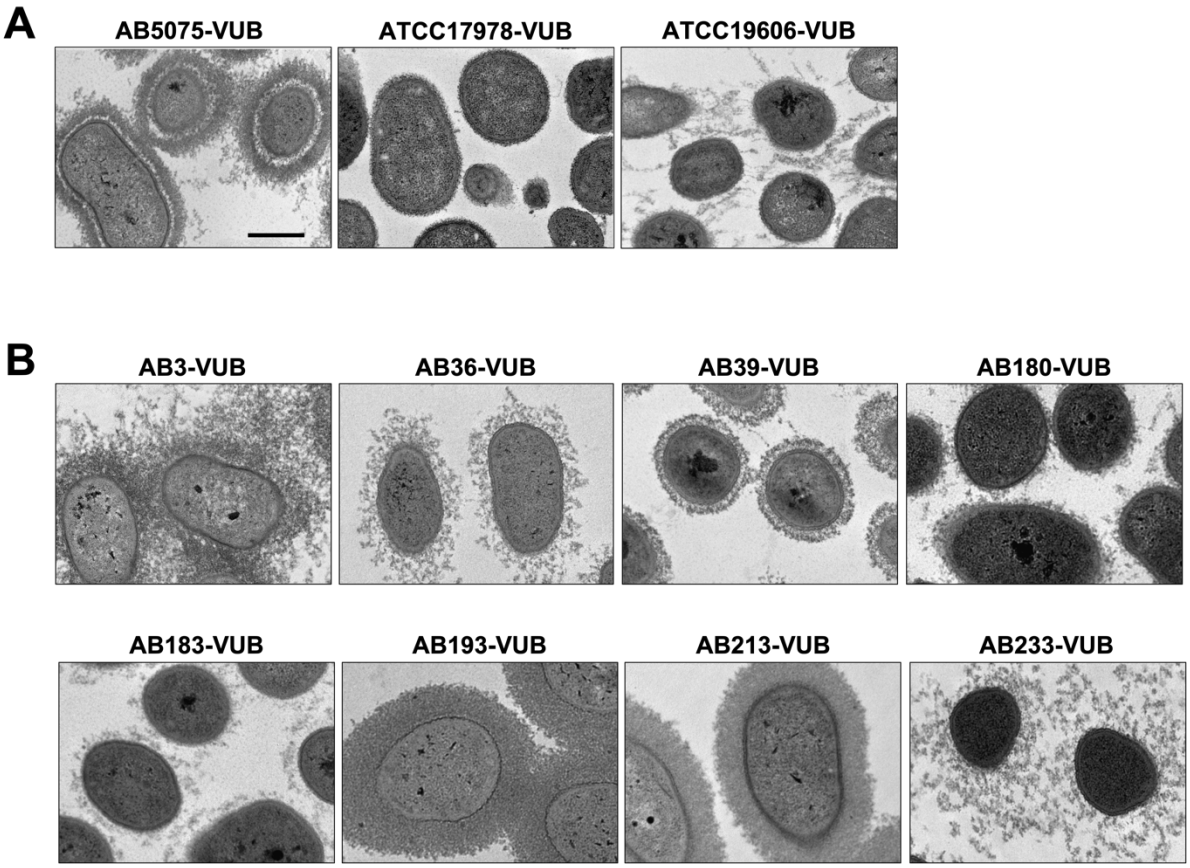

389

390 **Figure 5:** A TEM direct capsule visualization of three reference strains (A) and 8 modern clinical strains (B) of

391 various cell densities. Scale bar: 500 nm.

392

393 **Constitutive mucoid strains are not hyper-virulent**

394 As constitutive mucoid strains were observed only amongst the group of the modern MDR

395 clinical isolates, we wondered if this phenotype could be associated with a higher *in vivo*

396 virulence potential. *Galleria mellonella* larvae were infected with highly, medium, and weakly

397 capsulated isolates, while the AB5075-VUB reference strain was used as a positive control of

398 virulence (Jacobs et al., 2014). Concerning the constitutive mucoid isolates, while the AB213-

399 VUB is highly virulent, the constitutive mucoid isolates AB3-VUB and AB233-VUB are

400 weakly virulent (Figure 6). The medium capsulated isolate AB39-VUB was highly virulent and

401 killed 100% of the larvae within one day, being even more virulent than the AB5075-VUB,

while the medium capsulated AB36-VUB showed an intermediary virulence level. Interestingly, the low capsulated isolates (AB183-VUB and AB180-VUB) were the less virulent, AB180-VUB being avirulent in the tested conditions (Figure 6). These data show that a constitutive high capsulation and mucoid phenotype does not correlate with a higher virulence potential in *A. baumannii*. However, this highlights that low capsulation levels characterizes weakly virulent phenotypes, showing that *A. baumannii* bacteria required capsule deposition for full virulence. This is in agreement with previous studies showing that genetically manipulated capsule deficient *A. baumannii* strains have decreased virulence levels (Talyansky et al., 2021; Whiteway et al., 2021). As the virulence does not directly correlate with a specific KL or OCL type, we can conclude that the KL or OCL are not solely responsible for *A. baumannii* virulence in the tested conditions, which might require multifactorial influence. Taken together, these observations show that the reference strain AB5075 is a good bacterial model to study the virulence potential in *G. mellonella* while the less virulent strains ATCC19606 and ATCC17978 may be used in studies tackling down the modern clinical isolates exhibiting decreased virulence in *G. mellonella*.

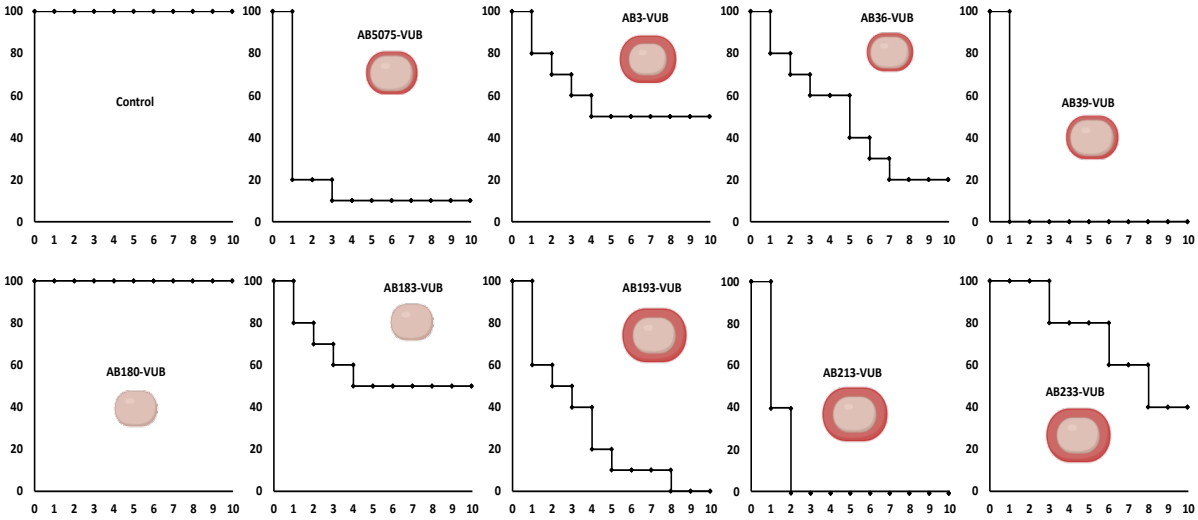

Figure 6: *In vivo* virulence of several modern *A. baumannii* isolates determined in *G. mellonella* model. X axis,

420 days after inoculation and Y axis, percentage of living *G. mellonella*. The control condition is the PS without
421 bacteria.
422

423 Discussion

424 The 43 modern MDR clinical isolates and four reference strains of *A. baumannii* were whole-
425 genome sequenced, *de novo* assembled and analyzed in the context of genotype and phenotype.
426 We identified 12 different ST groups in our collection of 43 modern clinical isolates. While the
427 reference strain AB5075-VUB belonged to less frequently occurring ST1 the reference strains
428 ATCC19606-VUB (ST52), ATCC17978-VUB (ST437) and DSM30011-VUB (ST738) did not
429 reflect the current trends of ST in clinical settings but rather rare sequence types. The lack of
430 representation of the ST of the clinical isolates is expectable only in the case of DSM30011-
431 VUB as this strain has environmental origin (plant microbiota). The ST2 group, previously
432 described as one important and clinically relevant group is also the most widely disseminated
433 ST among the complete and draft genomes available (Hamidian and Nigro, 2019). Most of the
434 modern clinical isolates of our collection belonged to ST2, yet none of the reference strains
435 represented this sequence type.
436 Our phylogenetic analysis (Figure 1) identified several clades, mostly in accordance with the
437 ST of the isolates. However, the reference strains DSM30011-VUB, ATCC17978-VUB and
438 ATCC19606-VUB formed a cluster with the least abundant sequence types of the clinical
439 isolates of *A. baumannii* [except AB226-VUB (ST604)]. Only this cluster consisted of the
440 isolates which all lacked *adeC* and *bauA* genes which are discussed below, suggesting an
441 extreme genetic diversity which represents only a minor proportion of the current clinical
442 isolates of *A. baumannii*. On the other hand, from the four reference strains, only AB5075-VUB
443 was the most similar to the modern clinical strains of *A. baumannii* in regard to OCL and
444 virulence genes. When considering AB5075-VUB capsule production, its phenotype was

445 resembling phenotypes of the clinical isolates with low production. Nevertheless, similarly to
446 the other reference strains, it lacked *bauA* and *adeC*. The lack of the combination of these two
447 virulence genes was also detected in ten modern clinical isolates proving that AB5075-VUB
448 still shares partial similarity with circulating clinical strains of *A. baumannii*. The described and
449 listed virulence genes in our study only account for a small amount of the virulence genes as
450 only known can be detected and possibly novel virulence genes remain to be identified.
451 Noteworthy, regardless of observed discrepancy in detection of *adeFGH* operon using VFDB
452 2022 and MEGARes 2.0 databases, the absence of *adeFGH* was described previously (Ardehali
453 et al., 2019; Coyne et al., 2010).
454 Capsule heterogeneity is a landmark of *A. baumannii* bacteria. The surface polysaccharides
455 play key roles in fitness and virulence of *A. baumannii* and protects it from the environment,
456 increases resistance to antimicrobial compounds and helps to evade the host immune system
457 (Geisinger and Isberg, 2015; Weber et al., 2016). There are more than 137 KL types identified
458 so far (Kenyon and Hall, 2021), and this variability demonstrates the diversity which must be
459 surveilled in the modern clinical isolates as the capsular polysaccharide is a potential target for
460 therapeutical agents and vaccines (Yang et al., 2017). In our collection of 43 modern clinical
461 isolates of MDR *A. baumannii*, KL40 (10/43) dominated while KL3 was detected in five
462 isolates.
463 In our study, the most prevalent locus encoding outer-core lipooligosaccharide (OCL) type in
464 the modern clinical isolates of MDR *A. baumannii* was OCL1 (31/43). However, none of the
465 reference strains represented this most prevalent OCL1 type as they belonged to OCL2
466 (AB5075-VUB and ATCC17978-VUB), OCL3 (ATCC19606-VUB) and OCL6 (DSM30011-
467 VUB) suggesting their rarefaction in following the current epidemiological trends.
468 Two reference strains (DSM30011-VUB and AB5075-VUB) in this study lacked *bap* gene
469 encoding biofilm associated protein which could influence the studies exploring biofilm

properties using these reference strains. However, the gene *bap* was found in ATCC17978-VUB and ATCC19606-VUB with 86% identity (VFDB 2022) same as in three clinical isolates (AB40-VUB, AB32-VUB and AB21-VUB), therefore assigned as undetected in the Figure 1 as the identity falls under the applied threshold if 90%. The *bap* encodes protein required for formation of three-dimensional biofilm towers and water channels on abiotic and biotic surfaces such as polypropylene, polystyrene, and titanium (Brossard and Campagnari, 2012). Bap protein is also involved in adherence of *A. baumannii* to human bronchial epithelial cells and human neonatal keratinocytes (Brossard and Campagnari, 2012). Moreover, nearly half of the examined strains (20/47) including four reference strain did not carry *bauA* encoding iron-regulated outer membrane protein BauA. BauA protein provides protection against sepsis caused by *A. baumannii* and was also identified as a vaccine candidate (Aghajani et al., 2019; Ni et al., 2017). Interestingly, six strains (including two reference strains DSM30011-VUB, ATCC19606-VUB and four clinical isolates AB177-VUB, AB186-VUB, AB40-VUB and AB21-VUB) encoded membrane fusion protein MexE protein, part of RND efflux pump from *Pseudomonas aeruginosa* (Köhler et al., 1999). Notably, the very same six strains were lacking a gene encoding membrane fusion protein AdeF from AdeFGH RND efflux pump, possibly restoring its function as AdeF and MexE share 50% homology. However, using the VFDB 2022 database, all clinical isolates and reference strains encoded *adeFGH* operon.

The deficiency of the clinical isolates and the reference strains in hemolytic and protease activities is in agreement with the fact that only some species of *Acinetobacter* genus, e.g., *Acinetobacter haemolyticus* (Touchon et al., 2014) are capable of such phenotype. Even despite this shared phenotypical trait, there was a high level of diversity of macrocolonies, where the reference strains represented only two variants out of five types observed in the clinical strains. Several modern isolates show a constitutive mucoid phenotype that is not observed in the reference strains. Isolates belonging to the same clusters (Figure 1) do not show the same

ultrastructure, showing a high diversity even within the same phylogenetic group. To be noted, also external events such as gene disruption can affect the phenotype of the macrocolony, as was observed in AB5075-UW by Perez-Varela (Pérez-Varela et al., 2020) by disrupting *relA* ortholog (*ABUW_3302*) using transposon insertion. Taken together, this points out the insufficiency of the reference strains in grasping the complete phenotypical (and genotypical) diversity of the modern clinical isolates.

The natural competence for transformation is one of the ways of horizontal gene transfer *A. baumannii* uses to acquire extracellular DNA from the environment and incorporates it into its own genome via homologous recombination (Dubnau and Blokesch, 2019). We observed that the competence to be naturally transformed varied within clinical isolates of *A. baumannii* from which 13 were transformed, 18 were not and 12 were intrinsically resistant to apramycin, therefore unable to assess. This diverse trend was copied by the reference strains as well as AB5075-VUB and DSM30011-VUB were successfully transformed while ATCC17978-VUB was not and ATCC19696-VUB showed intrinsic resistance to apramycin. There are multiple factors influencing the ability of *A. baumannii* to be naturally transformed such as presence of the H-NS (Le et al., 2021) which was present in each case within our isolates and strains. However, the major role is played by type IV pilus genes (Leong et al., 2017) which are growth phase dependent (Vesel and Blokesch, 2021), and might be the explanation of some isolates and strains not being transformed. However, the tested conditions of natural competence were standardized pointing out further physiological diversity within *A. baumannii* clinical isolates and reference strains. Despite the proven relevance of the clinical isolates of our collection (collected as problematic and modern nosocomial isolates), we cannot rule out a bias to certain extend.

We observe a high diversity in production of the capsular polysaccharide using direct and indirect visualization methods. We show a correlation between capsule abundance and density

levels, but correlation does not mean causation. We cannot rule out the possibility that the capsule type *per se* (and not only the capsule abundance) or other factors, influence the density of *A. baumannii* bacteria. The fact that widely used reference strains show low to medium encapsulation degrees add an additional reason why reference strains should be carefully used and argue in favor of considering the strain AB5075-VUB as the best representative bacterial model out of the four reference strains tested in this study. However, a rather complex solution to selection of proper strain to be used in a specific study is needed such as Acinetobase (Valcek et al., 2022). Acinetobase is a comprehensive database providing the community with genotype, phenotype and the strain of *A. baumannii* itself.

The *Galleria mellonella* infection model proved itself as a valuable source of information on the virulence level of *A. baumannii*. This model also highlighted AB5075-VUB to be more virulent than ATCC19606-VUB and ATCC17978-VUB in the tested conditions (Jacobs et al., 2014). These results support the usage of modern clinical isolates for study of virulence, hence other highly virulent isolates such as hypervirulent *A. baumannii* LAC-4 (Ou et al., 2015) should be considered as well.

As constitutive mucoid strains were observed only amongst the group of the modern MDR clinical isolates, we wondered if this phenotype could be associated with a higher *in vivo* virulence potential. The virulence in *G. mellonella* model varied for the tested clinical isolates and the reference strains and while a constitutive mucoid phenotype does not correlate with a higher virulence, we confirm using modern clinical isolates that low capsule production impedes full virulence in *A. baumannii*. These observations do not confirm the results of Shan et al., (Shan et al., 2021) who concluded that the mucoid *A. baumannii* isolates were more hypervirulent than the nonmucoid strains. This discrepancy may point towards multifactorial background of hypervirulence.

The signal(s) or conditions regulating capsule production remain to be determined. Noteworthy, the isolates AB193-VUB and AB213-VUB with higher integrity of the CPS layer (Figure 5) have shown higher virulence in *G. mellonella* (Figure 6) than isolates with dispersed CPS. The study of genetic features which are not shared by the majority of *A. baumannii* isolates (soft-core, shell and cloud genes (Cummins et al., 2022)) may lead to novel discoveries as well. However, the global impact of the clinical importance (drug therapies or target-driven drug discoveries) will suffer from linking the specific genes and features only to certain isolate or lineage.

Conclusion

A. baumannii are heterogenous bacteria, both at the genetic and phenotypic levels. In this study, we characterized 43 modern clinical isolates from different phylogenetic groups and 4 reference strains with common but also very different behaviors. Therefore, the reference strains tested in our study do not cover the whole heterogeneity found in the modern isolates of *A. baumannii*. The studies previously published using these reference strains built a strong state of the art in the *A. baumannii* field and beyond, showing their usefulness. However, the data presented in our study show that the specific use of one or only a limited subset of reference strains can hinder important processes characterizing clinically relevant isolates and the *A. baumannii* bacteria as a whole. As an answer to that identified pitfall, we propose a variable collection of modern clinical isolates that are characterized at the genetic and phenotypic levels, covering the full range of the phenotypic spectrum, with five different macrocolony type groups, from avirulent to hyper virulent phenotype, and with non-capsulated to hyper mucoid strains, with intermediate phenotypes as well. This will allow selecting a reference strain rationally, facilitated by the new Acinetobase (Valcek et al., 2022) platform, which suits the needs of an ongoing study with a particular biological question. This is especially important for new

569 antimicrobial screening purposes, for which conserved targets amongst a significant proportion
570 of problematic *A. baumannii* isolates is a prerequisite. While strain specific observation remains
571 interesting *per se*, in the context of such a drastic heterogeneity, any new identified target,
572 antimicrobial compound, or fundamental observation deserved to be tested on diverse relevant
573 *A. baumannii* isolates.
574
575
576
577
578

579 # Data availability

580 The long- and short-read sequences were deposited in GenBank under BioProject
581 PRJNA701627, PRJNA798866 and PRJNA734485, respectively.
582

583 # Funding

584 This project was supported by the Flanders Institute for Biotechnology (VIB) and has received
585 funding from the European Union's Horizon 2020 research and innovation program under the
586 Marie Sklodowska-Curie grant agreement No 748032. KN was supported by the Erasmus +
587 program KA131-HED.
588

589 # Acknowledgements

590 We are grateful to the URBM and URBE research groups, as well as the Electron Microscopy
591 Service from UNamur, for the access to their equipment and their expertise. We thank Ivan
592 Mateus from the Department of Ecology and Evolution, University of Lausanne, Lausanne,

Switzerland for a fruitful discussion of initial bioinformatical analyses. We thank the National Reference Laboratory for Monitoring of Antimicrobial Resistance in Gram-negative Bacteria, CHU Mont-Godinne, Université Catholique de Louvain (UCL), Yvoir (Belgium) for providing the modern clinical isolates.

Competing interests

None to declare.

Contribution

CP, CVDH and ER performed phenotypical experiments. AV, CVDH and KN performed bioinformatical analyses. CW extracted DNA for the long-read sequencing. MB, CP, CVDH and TC performed the infections of *Galleria mellonella*. TDP, WDC and MS set up the LRS strategy, sample, library preparation and sequencing. JK provided her expertise in KL and OCL identification. AV and CVDH wrote the manuscript.

References

Aghajani Z, Rasooli I, Mousavi Gargari SL. 2019. Exploitation of two siderophore receptors, BauA and BfnH, for protection against *Acinetobacter baumannii* infection. *APMIS* **127**:753–763. doi:10.1111/apm.12992

Arbatsky NP, Shneider MM, Kenyon JJ, Shashkov AS, Popova A v., Miroshnikov KA, Volozhantsev N v., Knirel YA. 2015. Structure of the neutral capsular polysaccharide of *Acinetobacter baumannii* NIPH146 that carries the KL37 capsule gene cluster. *Carbohydrate Research* **413**:12–15. doi:10.1016/J.CARRES.2015.05.003

Ardehali SH, Azimi T, Fallah F, Owrang M, Aghamohammadi N, Azimi L. 2019. Role of efflux pumps in reduced susceptibility to tigecycline in *Acinetobacter baumannii*. *New Microbes and New Infections* **30**:100547. doi:10.1016/J.NMNI.2019.100547

Ardissone S, Fumeaux C, Bergé M, Beaussart A, Théraulaz L, Radhakrishnan SK, Dufrêne YF, Viollier PH. 2014. Cell cycle constraints on capsulation and bacteriophage susceptibility. *eLife* **3**:1–30. doi:10.7554/ELIFE.03587

623 Bolger AM, Lohse M, Usadel B. 2014. Trimmomatic: A flexible trimmer for Illumina sequence
624 data. *Bioinformatics* **30**:2114–2120. doi:10.1093/bioinformatics/btu170
625 Bortolaia V, Kaas RS, Ruppe E, Roberts MC, Schwarz S, Cattoir V, Philippon A, Allesoe RL,
626 Rebelo AR, Florensa AF, Fagelhauer L, Chakraborty T, Neumann B, Werner G, Bender
627 JK, Stingl K, Nguyen M, Coppens J, Xavier BB, Malhotra-Kumar S, Westh H, Pinholt M,
628 Anjum MF, Duggett NA, Kempf I, Nykäsenoja S, Olkkola S, Wieczorek K, Amaro A,
629 Clemente L, Mossong J, Losch S, Ragimbeau C, Lund O, Aarestrup FM. 2020. ResFinder
630 4.0 for predictions of phenotypes from genotypes. *Journal of Antimicrobial Chemotherapy*
631 **75**:3491–3500. doi:10.1093/JAC/DKAA345
632 Bouvet PJM, Grimont PAD. 1986. Taxonomy of the Genus *Acinetobacter* with the Recognition
633 of *Acinetobacter baumannii* sp. nov., *Acinetobacter haemolyticus* sp. nov., *Acinetobacter*
634 *johnsonii* sp. nov., and *Acinetobacter junii* sp. nov. and Emended Descriptions of
635 *Acinetobacter calcoaceticus* and *Acinetobacter lwoffii*. *International Journal of*
636 *Systematic and Evolutionary Microbiology* **36**:228–240. doi:10.1099/00207713-36-2-228
637 Bravo Z, Orruño M, Parada C, Kaberdin VR, Barcina I, Arana I. 2016. The long-term survival
638 of *Acinetobacter baumannii* ATCC 19606T under nutrient-deprived conditions does not
639 require the entry into the viable but non-culturable state. *Archives of Microbiology*
640 **198**:399–407. doi:10.1007/s00203-016-1200-1
641 Brossard KA, Campagnari AA. 2012. The *Acinetobacter baumannii* Biofilm-Associated
642 Protein Plays a Role in Adherence to Human Epithelial Cells. doi:10.1128/IAI.05913-11
643 Centers for Disease Control and Prevention (U.S.);National Center for Emerging Zoonotic and
644 Infectious Diseases (U.S.). Division of Healthcare Quality Promotion. Antibiotic
645 Resistance Coordination and Strategy Unit. 2019. Antibiotic Resistance Threats in the
646 United States, 2019. doi:10.15620/cdc:82532
647 Chiang SR, Jung F, Tang HJ, Chen CH, Chen CC, Chou HY, Chuang YC. 2018. Desiccation
648 and ethanol resistances of multidrug resistant *Acinetobacter baumannii* embedded in
649 biofilm: The favorable antiseptic efficacy of combination chlorhexidine gluconate and
650 ethanol. *Journal of Microbiology, Immunology and Infection* **51**:770–777.
651 doi:10.1016/j.jmii.2017.02.003
652 Chin CY, Tipton KA, Farokhyfar M, Burd EM, Weiss DS, Rather PN. 2018. A high-frequency
653 phenotypic switch links bacterial virulence and environmental survival in *Acinetobacter*
654 *baumannii*. *Nature Microbiology 2018 3:5* **3**:563–569. doi:10.1038/s41564-018-0151-5
655 Coyne S, Rosenfeld N, Lambert T, Courvalin P, Périchon B. 2010. Overexpression of
656 resistance-nodulation-cell division pump AdeFGH confers multidrug resistance in
657 *Acinetobacter baumannii*. *Antimicrobial Agents and Chemotherapy* **54**:4389–4393.
658 doi:10.1128/AAC.00155-10/ASSET/051BDFEF-DB1A-4F55-B6EB-
659 323DD38348B4/ASSETS/GRAPHIC/ZAC9991093410002.JPEG
660 Cummins EA, Hall RJ, McInerney JO, McNally A. 2022. Prokaryote pangenomes are dynamic
661 entities. *Current Opinion in Microbiology* **66**:73–78. doi:10.1016/J.MIB.2022.01.005
662 da Silva G, Domingues S. 2016. Insights on the Horizontal Gene Transfer of Carbapenemase
663 Determinants in the Opportunistic Pathogen *Acinetobacter baumannii*. *Microorganisms*
664 **4**:29. doi:10.3390/microorganisms4030029
665 de Coster W, D'hert S, Schultz DT, Cruts M, van Broeckhoven C. 2018. NanoPack: visualizing
666 and processing long-read sequencing data. doi:10.1093/bioinformatics/bty149
667 de Oliveira DMP, Forde BM, Kidd TJ, Harris PNA, Schembri MA, Beatson SA, Paterson DL,
668 Walker MJ. 2020. Antimicrobial Resistance in ESKAPE Pathogens. doi:10.1128/CMR
669 de Silva PM, Chong P, Fernando DM, Westmacott G, Kumar A. 2017. Effect of Incubation
670 Temperature on Antibiotic Resistance and Virulence Factors of *Acinetobacter baumannii*
671 ATCC 17978. doi:10.1128/AAC.01514-17

672 Dong C, Beis K, Nesper J, Brunkan AL, Clarke BR, Whitfield C, Naismith JH. 2006. The
673 structure of Wza, the translocon for group 1 capsular polysaccharides in *Escherichia coli*,
674 identifies a new class of outer membrane protein. *Nature* **444**:226.
675 doi:10.1038/NATURE05267
676 Doster E, Lakin SM, Dean CJ, Wolfe C, Young JG, Boucher C, Belk KE, Noyes NR, Morley
677 PS. 2020. MEGARes 2.0: A database for classification of antimicrobial drug, biocide and
678 metal resistance determinants in metagenomic sequence data. *Nucleic Acids Research*
679 **48**:D561–D569. doi:10.1093/nar/gkz1010
680 Dubnau D, Blokesch M. 2019. Mechanisms of DNA Uptake by Naturally Competent Bacteria.
681 *https://doi.org/101146/annurev-genet-112618-043641* **53**:217–237.
682 doi:10.1146/ANNUREV-GENET-112618-043641
683 Gaiarsa S, Batisti Biffignandi G, Esposito EP, Castelli M, Jolley KA, Brisse S, Sassera D,
684 Zarrilli R. 2019. Comparative analysis of the two *Acinetobacter baumannii* multilocus
685 sequence typing (MLST) schemes. *Frontiers in Microbiology* **10**.
686 doi:10.3389/fmicb.2019.00930
687 Gallagher LA, Ramage E, Weiss EJ, Radey M, Hayden HS, Held KG, Huse HK, Zurawski D
688 v., Brittnacher MJ, Manoil C. 2015. Resources for genetic and genomic analysis of
689 emerging pathogen *Acinetobacter baumannii*. *Journal of Bacteriology* **197**:2027–2035.
690 doi:10.1128/JB.00131-15
691 Geisinger E, Huo W, Hernandez-Bird J, Isberg RR. 2019. *Acinetobacter baumannii*: Envelope
692 Determinants That Control Drug Resistance, Virulence, and Surface Variability.
693 *https://doi.org/101146/annurev-micro-020518-115714* **73**:481–506.
694 doi:10.1146/ANNUREV-MICRO-020518-115714
695 Geisinger E, Isberg RR. 2015. Antibiotic Modulation of Capsular Exopolysaccharide and
696 Virulence in *Acinetobacter baumannii*. *PLOS Pathogens* **11**:e1004691.
697 doi:10.1371/journal.ppat.1004691
698 Hamidian M, Nigro SJ. 2019. Emergence, molecular mechanisms and global spread of
699 carbapenem-resistant *Acinetobacter baumannii*. *Microbial Genomics*.
700 doi:10.1099/mgen.0.000306
701 Harding CM, Hennon SW, Feldman MF. 2017. Uncovering the mechanisms of *Acinetobacter*
702 *baumannii* virulence. *Nature Reviews Microbiology 2017 16:2* **16**:91–102.
703 doi:10.1038/nrmicro.2017.148
704 Hernando-Amado S, Coque TM, Baquero F, Martínez JL. 2019. Defining and combating
705 antibiotic resistance from One Health and Global Health perspectives. *Nature*
706 *Microbiology*. doi:10.1038/s41564-019-0503-9
707 Holley G, Beyter D, Ingimundardottir H, Møller PL, Kristmundsdottir S, Eggertsson HP,
708 Halldorsson B v. 2021. Ratatosk: hybrid error correction of long reads enables accurate
709 variant calling and assembly. *Genome Biology* **22**:1–22. doi:10.1186/S13059-020-02244-
710 4/FIGURES/8
711 Imperi F, Antunes LCS, Blom J, Villa L, Iacono M, Visca P, Carattoli A. 2011. The genomics
712 of *Acinetobacter baumannii*: Insights into genome plasticity, antimicrobial resistance and
713 pathogenicity. *IUBMB Life* **63**:1068–1074. doi:10.1002/iub.531
714 Jacobs AC, Thompson MG, Black CC, Kessler JL, Clark LP, McQueary CN, Gancz HY, Corey
715 BW, Moon JK, Si Y, Owen MT, Hallock JD, Kwak YI, Summers A, Li CZ, Rasko DA,
716 Penwell WF, Honnold CL, Wise MC, Waterman PE, Lesho EP, Stewart RL, Actis LA,
717 Palys TJ, Craft DW, Zurawski D v. 2014. AB5075, a highly virulent isolate of
718 *Acinetobacter baumannii*, as a model strain for the evaluation of pathogenesis and
719 antimicrobial treatments. *mBio* **5**. doi:10.1128/mBio.01076-14

720 Kenyon JJ, Hall RM. 2021. Updated Analysis of the Surface Carbohydrate Gene Clusters in a
721 Diverse Panel of *Acinetobacter baumannii* Isolates. *Antimicrobial Agents and*
722 *Chemotherapy* **66**. doi:10.1128/AAC.01807-21
723 Kenyon JJ, Hall RM. 2013. Variation in the Complex Carbohydrate Biosynthesis Loci of
724 *Acinetobacter baumannii* Genomes. *PLoS ONE* **8**:e62160.
725 doi:10.1371/journal.pone.0062160
726 Kenyon JJ, Nigro SJ, Hall RM. 2014. Variation in the OC Locus of *Acinetobacter baumannii*
727 Genomes Predicts Extensive Structural Diversity in the Lipooligosaccharide. *PLoS ONE*
728 **9**:e107833. doi:10.1371/journal.pone.0107833
729 Köhler T, Epp SF, Curty LK, Pechère JC. 1999. Characterization of MexT, the regulator of the
730 MexE-MexF-OprN multidrug efflux system of *Pseudomonas aeruginosa*. *Journal of*
731 *Bacteriology* **181**:6300–6305. doi:10.1128/jb.181.20.6300-6305.1999
732 Kolmogorov M, Yuan J, Lin Y, Pevzner PA. 2019. Assembly of long, error-prone reads using
733 repeat graphs. *Nature Biotechnology* **37**:540–546. doi:10.1038/s41587-019-0072-8
734 Kon H, Schwartz D, Temkin E, Carmeli Y, Lellouche J. 2020. Rapid identification of
735 capsulated *Acinetobacter baumannii* using a density-dependent gradient test. *BMC*
736 *Microbiology* **20**:1–11. doi:10.1186/s12866-020-01971-9
737 Le C, Pimentel C, Tuttobene MR, Subils T, Escalante J, Nishimura B, Arriaga S, Rodgers D,
738 Bonomo RA, Sieira R, Tolmasky ME, Ramírez MS. 2021. Involvement of the Histone-
739 Like Nucleoid Structuring Protein (H-NS) in *Acinetobacter baumannii*'s Natural
740 Transformation. *Pathogens 2021, Vol 10, Page 1083* **10**:1083.
741 doi:10.3390/PATHOGENS10091083
742 Leong CG, Bloomfield RA, Boyd CA, Dornbusch AJ, Lieber L, Liu F, Owen A, Slay E, Lang
743 KM, Lostroh CP. 2017. The role of core and accessory type IV pilus genes in natural
744 transformation and twitching motility in the bacterium *Acinetobacter baylyi*. *PLOS ONE*
745 **12**:e0182139. doi:10.1371/JOURNAL.PONE.0182139
746 Letunic I, Bork P. 2019. Interactive Tree of Life (iTOL) v4: Recent updates and new
747 developments. *Nucleic Acids Research* **47**:W256–W259. doi:10.1093/nar/gkz239
748 Liu B, Zheng D, Zhou S, Chen L, Yang J. 2022. VFDB 2022: a general classification scheme
749 for bacterial virulence factors. *Nucleic Acids Research* **50**:D912–D917.
750 doi:10.1093/NAR/GKAB1107
751 Murray CJ, Ikuta KS, Sharara F, Swetschinski L, Robles Aguilar G, Gray A, Han C, Bisignano
752 C, Rao P, Wool E, Johnson SC, Browne AJ, Chipeta MG, Fell F, Hackett S, Haines-
753 Woodhouse G, Kashef Hamadani BH, Kumaran EAP, McManigal B, Agarwal R, Akech
754 S, Albertson S, Amuasi J, Andrews J, Aravkin A, Ashley E, Bailey F, Baker S, Basnyat
755 B, Bekker A, Bender R, Bethou A, Bielicki J, Boonkasidecha S, Bukosia J, Carvalheiro
756 C, Castañeda-Orjuela C, Chansamouth V, Chaurasia S, Chiurchiù S, Chowdhury F, Cook
757 AJ, Cooper B, Cressey TR, Criollo-Mora E, Cunningham M, Darboe S, Day NPJ, de Luca
758 M, Dokova K, Dramowski A, Dunachie SJ, Eckmanns T, Eibach D, Emami A, Feasey N,
759 Fisher-Pearson N, Forrest K, Garrett D, Gastmeier P, Giref AZ, Greer RC, Gupta V, Haller
760 S, Haselbeck A, Hay SI, Holm M, Hopkins S, Iregbu KC, Jacobs J, Jarovsky D,
761 Javanmardi F, Khorana M, Kissoon N, Kobeissi E, Kostyanev T, Krapp F, Krumkamp R,
762 Kumar A, Kyu HH, Lim C, Limmathurotsakul D, Loftus MJ, Lunn M, Ma J, Mturi N,
763 Munera-Huertas T, Musicha P, Mussi-Pinhata MM, Nakamura T, Nanavati R, Nangia S,
764 Newton P, Ngoun C, Novotney A, Nwakanma D, Obiero CW, Olivas-Martinez A, Olliaro
765 P, Ooko E, Ortiz-Brizuela E, Peleg AY, Perrone C, Plakkal N, Ponce-de-Leon A, Raad M,
766 Ramdin T, Riddell A, Roberts T, Robotham JV, Roca A, Rudd KE, Russell N, Schnall J,
767 Scott JAG, Shivamallappa M, Sifuentes-Osornio J, Steenkeste N, Stewardson AJ, Stoeva
768 T, Tasak N, Thaiprakong A, Thwaites G, Turner C, Turner P, van Doorn HR, Velaphi S,
769 Vongpradith A, Vu H, Walsh T, Waner S, Wangrangsimakul T, Wozniak T, Zheng P,

Sartorius B, Lopez AD, Stergachis A, Moore C, Dolecek C, Naghavi M. 2022. Global burden of bacterial antimicrobial resistance in 2019: a systematic analysis. *The Lancet* **399**:629–655. doi:10.1016/S0140-6736(21)02724-0

Ni Z, Chen Y, Ong E, He Y. 2017. Antibiotic resistance determinant-focused *Acinetobacter baumannii* vaccine designed using reverse vaccinology. *International Journal of Molecular Sciences* **18**. doi:10.3390/ijms18020458

Niu T, Guo L, Luo Q, Zhou K, Yu W, Chen Y, Huang C, Xiao Y. 2019. Wza gene knockout decreases *Acinetobacter baumannii* virulence and affects Wzy-dependent capsular polysaccharide synthesis. *https://doi.org/101080/2150559420191700659* **11**:1–13. doi:10.1080/21505594.2019.1700659

Ou HY, Kuang SN, He X, Molgora BM, Ewing PJ, Deng Z, Osby M, Chen W, Xu HH. 2015. Complete genome sequence of hypervirulent and outbreak-associated *Acinetobacter baumannii* strain LAC-4: epidemiology, resistance genetic determinants and potential virulence factors. *Scientific Reports 2015 5:1* **5**:1–13. doi:10.1038/srep08643

Page AJ, Cummins CA, Hunt M, Wong VK, Reuter S, Holden MTG, Fookes M, Falush D, Keane JA, Parkhill J. 2015. Roary: Rapid large-scale prokaryote pan genome analysis. *Bioinformatics* **31**:3691–3693. doi:10.1093/bioinformatics/btv421

Pérez-Varela M, Tierney ARP, Kim J-S, Vázquez-Torres A, Rather P. 2020. Characterization of RelA in *Acinetobacter baumannii*. doi:10.1128/JB.00045-20

Poirel L, Nordmann P. 2006. Carbapenem resistance in *Acinetobacter baumannii*: Mechanisms and epidemiology. *Clinical Microbiology and Infection*. doi:10.1111/j.1469-0691.2006.01456.x

Repizo GD, Viale AM, Borges V, Cameranesi MM, Taib N, Espariz M, Brochier-Armanet C, Gomes JP, Salcedo SP. 2017. The Environmental *Acinetobacter baumannii* Isolate DSM30011 Reveals Clues into the Preantibiotic Era Genome Diversity, Virulence Potential, and Niche Range of a Predominant Nosocomial Pathogen. *Genome Biology and Evolution* **9**:2292–2307. doi:10.1093/GBE/EVX162

Roussin M, Rabarioelina S, Cluzeau L, Cayron J, Lesterlin C, Salcedo SP, Bigot S. 2019. Identification of a Contact-Dependent Growth Inhibition (CDI) System That Reduces Biofilm Formation and Host Cell Adhesion of *Acinetobacter baumannii* DSM30011 Strain. *Frontiers in Microbiology* **10**:2450. doi:10.3389/fmicb.2019.02450

Seemann T. 2014. Prokka: Rapid prokaryotic genome annotation. *Bioinformatics* **30**:2068–2069. doi:10.1093/bioinformatics/btu153

Senchenkova SN, Shashkov AS, Popova A v., Shneider MM, Arbatsky NP, Miroshnikov KA, Volozhantsev N v., Knirel YA. 2015. Structure elucidation of the capsular polysaccharide of *Acinetobacter baumannii* AB5075 having the KL25 capsule biosynthesis locus. *Carbohydrate Research* **408**:8–11. doi:10.1016/J.CARRES.2015.02.011

Shan W, Zhang H, Kan J, Yin M, Zhang J, Wan L, Chang R, Li M. 2021. Acquired mucoid phenotype of *Acinetobacter baumannii*: Impact for the molecular characteristics and virulence. *Microbiological Research* **246**:126702. doi:10.1016/J.MICRES.2021.126702

Stamatakis A. 2006. RAxML-VI-HPC: Maximum likelihood-based phylogenetic analyses with thousands of taxa and mixed models. *Bioinformatics* **22**:2688–2690. doi:10.1093/bioinformatics/btl446

Tacconelli E, Carrara E, Savoldi A, Harbarth S, Mendelson M, Monnet DL, Pulcini C, Kahlmeter G, Kluytmans J, Carmeli Y, Ouellette M, Outterson K, Patel J, Cavaleri M, Cox EM, Houchens CR, Grayson L, Hansen P, Singh N, Theuretzbacher U, Magrini N. 2018. Discovery, research, and development of new antibiotics: the WHO priority list of antibiotic-resistant bacteria and tuberculosis. *www.thelancet.com/infection* **18**. doi:10.1016/S1473-3099(17)30753-3

Talyansky Y, Nielsen TB, Yan J, Carlino-Macdonald U, di Venanzio G, Chakravorty S, Ulhaq A, Feldman MF, Russo TA, Vinogradov E, Luna B, Wright MS, Adams MD, Spellberg B. 2021. Capsule carbohydrate structure determines virulence in *Acinetobacter baumannii*. *PLOS Pathogens* **17**:e1009291. doi:10.1371/JOURNAL.PPAT.1009291

Tipton KA, Dimitrova D, Rather PN. 2015. Phase-variable control of multiple phenotypes in *Acinetobacter baumannii* strain AB5075. *Journal of Bacteriology* **197**:2593–2599. doi:10.1128/JB.00188-15

Touchon M, Cury J, Yoon EJ, Krizova L, Cerqueira GC, Murphy C, Feldgarden M, Wortman J, Clermont D, Lambert T, Grillot-Courvalin C, Nemec A, Courvalin P, Rocha EPC. 2014. The genomic diversification of the whole *Acinetobacter* genus: Origins, mechanisms, and consequences. *Genome Biology and Evolution* **6**:2866–2882. doi:10.1093/gbe/evu225

Valcek A, Bogaerts P, Denis O, Huang T-D, Van der Henst C. 2021. Molecular epidemiology of carbapenem-resistant *Acinetobacter baumannii* strains in Belgian acute-care hospitals. *medRxiv* 2021.07.06.21259728. doi:10.1101/2021.07.06.21259728

Valcek A, Collier J, Botzki A, Henst C van der. 2022. Acinetobase: the comprehensive database and repository of *Acinetobacter* strains. *bioRxiv* 2022.02.27.482141. doi:10.1101/2022.02.27.482141

Van der Henst C, Vanhove AS, Drebes Dörr NC, Stutzmann S, Stoudmann C, Clerc S, Scrignari T, Maclachlan C, Knott G, Blokesch M. 2018. Molecular insights into *Vibrio cholerae*'s intra-amoebal host-pathogen interactions. *Nature Communications 2018 9:1* **9**:1–13. doi:10.1038/s41467-018-05976-x

Vesel N, Blokesch M. 2021. Pilus Production in *Acinetobacter baumannii* Is Growth Phase Dependent and Essential for Natural Transformation. doi:10.1128/JB.00034-21

Walker BJ, Abeel T, Shea T, Priest M, Abouelliel A, Sakthikumar S, Cuomo CA, Zeng Q, Wortman J, Young SK, Earl AM. 2014. Pilon: An Integrated Tool for Comprehensive Microbial Variant Detection and Genome Assembly Improvement. *PLoS ONE* **9**:e112963. doi:10.1371/journal.pone.0112963

Wang-Lin SX, Olson R, Beanan JM, MacDonald U, Balthasar JP, Russo TA. 2017. The Capsular Polysaccharide of *Acinetobacter baumannii* Is an Obstacle for Therapeutic Passive Immunization Strategies. *Infection and Immunity* **85**. doi:10.1128/IAI.00591-17

Weber BS, Harding CM, Feldman MF. 2016. Pathogenic *Acinetobacter*: from the Cell Surface to Infinity and Beyond. doi:10.1128/JB.00906-15

Whiteway C, Breine A, Philippe C, Van der Henst C. 2022. *Acinetobacter baumannii*. *Trends in Microbiology* **30**:199–200. doi:10.1016/J.TIM.2021.11.008

Whiteway C, Valcek A, Philippe C, Strazisar M, de Pooter T, Mateus I, Breine A, Van der Henst C. 2021. Scarless excision of an insertion sequence restores capsule production and virulence in *Acinetobacter baumannii*. *The ISME Journal 2022* 1–5. doi:10.1038/s41396-021-01179-3

Wick RR, Heinz E, Holt KE, Wyres KL, Diekema DJ. 2018. Kaptive Web: User-Friendly Capsule and Lipopolysaccharide Serotype Prediction for *Klebsiella* Genomes. *jcm.asm.org 1 Journal of Clinical Microbiology* **56**:197–215. doi:10.1128/JCM.00197-18

Wyres KL, Cahill SM, Holt KE, Hall RM, Kenyon JJ. 2020. Identification of *Acinetobacter baumannii* loci for capsular polysaccharide (KL) and lipooligosaccharide outer core (OCL) synthesis in genome assemblies using curated reference databases compatible with kaptive. *Microbial Genomics* **6**:e000339. doi:10.1099/mgen.0.000339

Yang FL, Lou TC, Kuo SC, Wu WL, Chern J, Lee YT, Chen ST, Zou W, Lin NT, Wu SH. 2017. A medically relevant capsular polysaccharide in *Acinetobacter baumannii* is a potential vaccine candidate. *Vaccine* **35**:1440–1447. doi:10.1016/j.vaccine.2017.01.060

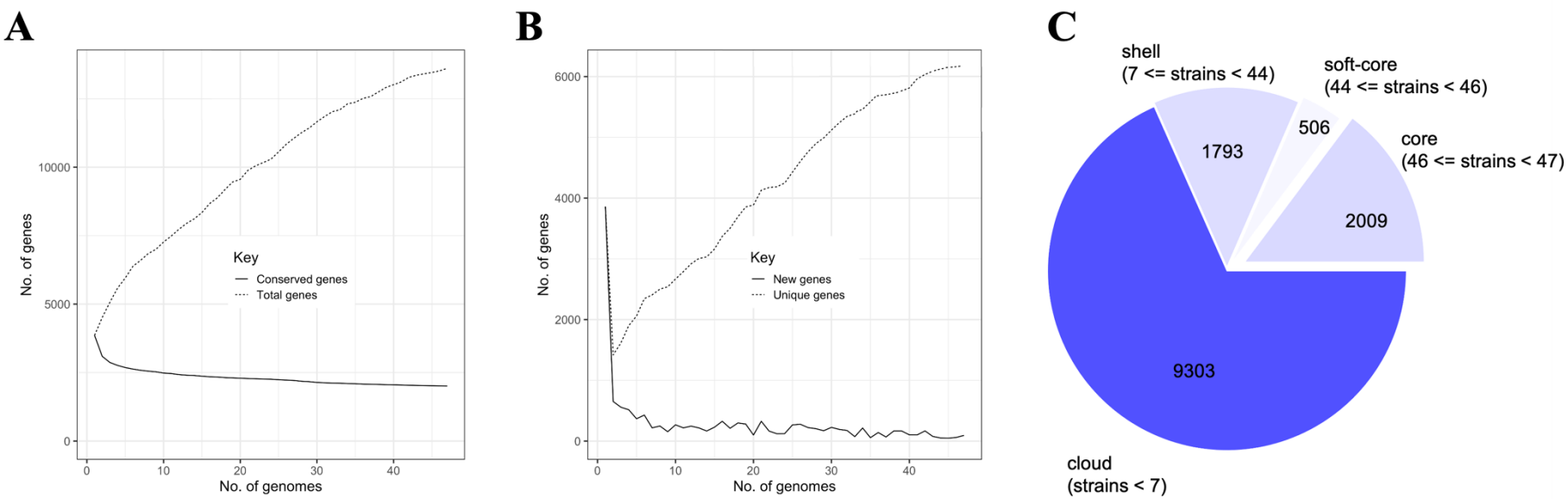

Figure 1: A depiction of (A) Conserved and total gene numbers in the pangenome. (B) Novel and unique gene numbers in the pangenome. These graphs indicate how the pangenome varies as genomes are added. (C) Pangenome pie chart showing the number of core and accessory genes. Accessory genes were divided into soft core, shell and cloud genes.

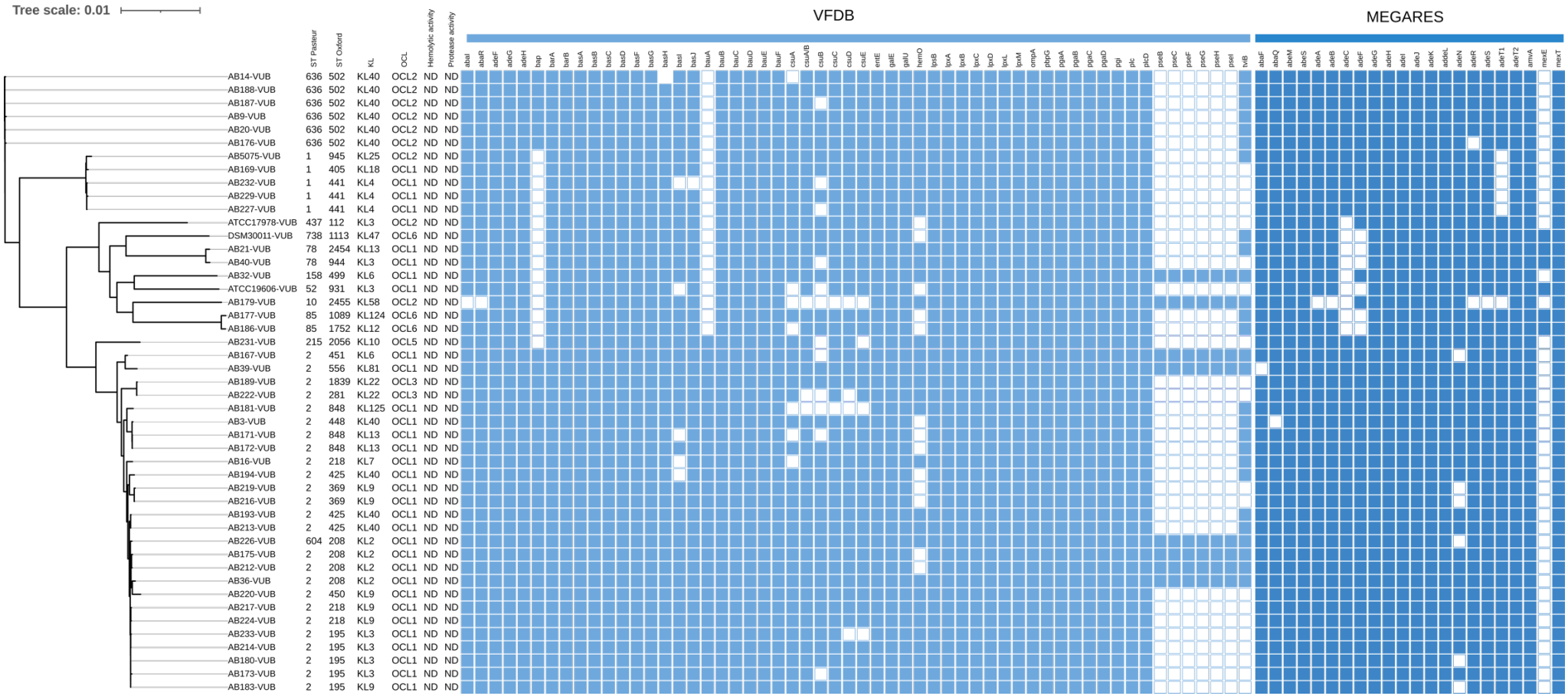

874

875 **Figure 2:** A phylogenetic tree of 43 modern clinical isolates and four reference strains of *A. baumannii* with depiction of ST^{Pas} and ST^{Ox}, KL, OCL, hemolytic activity, protease

876 activity and virulence genes as detected using VFDB 2022 and MEGARes 2.0 databases, respectively. ND – Not Detected

877

878 **Supplementary Figure 1:** A phylogenetic tree of 43 modern clinical isolates and four reference strains of *A. baumannii* with depiction of ST^{Pas} and ST^{Ox}, KL, OCL, hemolytic

879 activity, protease activity and resistance genes, respectively. ND – Not Detected